Annual Review of Physical Chemistry

Computational Design of Clusters for Catalysis

Elisa Jimenez-Izal[1,2] and Anastassia N. Alexandrova[1,3]

[1]Department of Chemistry and Biochemistry, University of California, Los Angeles, California 90095, USA

[2]Kimika Fakultatea, Euskal Herriko Unibertsitatea (UPV/EHU) and Donostia International Physics Center (DIPC), 20080 Donostia, Euskadi, Spain

[3]California NanoSystems Institute, Los Angeles, California 90095, USA; email: ana@chem.ucla.edu

Annu. Rev. Phys. Chem. 2018. 69:15.1–15.24

The *Annual Review of Physical Chemistry* is online at physchem.annualreviews.org

https://doi.org/10.1146/annurev-physchem-050317-014216

Keywords

nanoclusters, platinum, catalysis, DFT, fluxionality, realistic modeling

Abstract

When small clusters are studied in chemical physics or physical chemistry, one perhaps thinks of the fundamental aspects of cluster electronic structure, or precision spectroscopy in ultracold molecular beams. However, small clusters are also of interest in catalysis, where the cold ground state or an isolated cluster may not even be the right starting point. Instead, the big question is: What happens to cluster-based catalysts under real conditions of catalysis, such as high temperature and coverage with reagents? Myriads of metastable cluster states become accessible, the entire system is dynamic, and catalysis may be driven by rare sites present only under those conditions. Activity, selectivity, and stability are highly dependent on size, composition, shape, support, and environment. To probe and master cluster catalysis, sophisticated tools are being developed for precision synthesis, operando measurements, and multiscale modeling. This review intends to tell the messy story of clusters in catalysis.

1. INTRODUCTION

Catalysts have an enormous impact on the world economy. Today, over 90% of all chemical manufacturing processes make use of heterogeneous catalysis (1). These critical materials enable selective formation of desired products at rates that are commercially viable. Catalysis is not only important for the production of chemicals, materials, and food, but also essential for pollution control and medical applications, and it is at the heart of the development of sustainable energy solutions. Currently, the ultimate goal of research in heterogeneous catalysis is to provide a fundamental understanding of the processes involved in a catalytic reaction and to be able to design and synthesize catalysts with optimized properties (2).

The majority of industrial catalysts consist of transition metal particles dispersed on high–surface area supports (3). These nanoparticles typically have dimensions of a few nanometers. When the dimensions are further reduced to nanoclusters made of just a few atoms, many exciting possibilities emerge. Indeed, when matter is organized at the nanoscale, its behavior can be dramatically different from that of the bulk. Its properties become size-dependent, changing discontinuously with size. Two main factors are responsible for this phenomenon. First, when the wavelength of the electrons in the material is on the order of the material's size, quantum effects rule the behavior and properties of the system. Band structure becomes discontinuous and breaks down into discrete energy levels. The highest occupied molecular orbital (HOMO)–lowest unoccupied molecular orbital (LUMO) gaps, ionization potentials, electron affinities, etc. become size dependent. These same properties relate to the availability of electrons for forming bonds or being involved in reduction–oxidation reactions. Therefore, catalytic activity and selectivity become a function of size (4). Second, the high surface-to-volume ratio of nanoparticles plays an important role. As most of the atoms are at the surface of the structure, they rearrange themselves to minimize the number of dangling bonds and the surface energy, giving rise to unexpected structures. Because of these particularities, interesting and high catalytic activities often arise (5–20). Hence, heterogeneous catalysis has the potential to undergo a renaissance and to make possible many previously inaccessible industrial processes. Importantly, with dwindling supplies of precious metals and increasing demand, supported metallic nanoclusters (up to about 30 atoms) are key to achieving cheaper and "greener" industrial catalytic processes. These promising systems are the focus of this review.

Subnanocluster catalysts are extremely complex and present challenges for operando characterization, theoretical modeling, precision synthesis targeting the formation of the most critical sites, identification of the electronic and structural origins of special properties in realistic conditions, and eventual mastery at the level of design. The first investigationson metallic nanoclusters were done in the gas phase (21–25), although real industrial applicability lies in supported clusters and particles, and the support dramatically modifies their properties, as will be discussed in Section 5. Later, experimental techniques for cluster generation, size selection, and surface deposition (26–34) were developed, allowing the study of deposited clusters with precise numbers of atoms (35–37). These developments made it possible for researchers to approach an architecture that is tractable yet reasonable for catalysis applications. A wide variety of characterization methods, including scanning tunneling microscopy as well as ultraviolet and X-ray photoelectron spectroscopy, have become fundamental to determining structure–activity relationships (38–41). In addition, thanks to advances in software and hardware, size-selected nanoclusters deposited on oxides are now treatable by first-principles computational protocols. Indeed, for these systems, experiments rely heavily on computational investigations, and the synergy between experiment and computation has been critical for advancement in this field.

In this review, we discuss the major features of cluster catalysts, the promises and challenges that they offer, advances in our understanding of them, and progress in their design. We show how subtle changes in the size, support, temperature, and environment in a particular reaction

can dramatically alter cluster properties, changing the very nature of the catalyst. We discuss how size reduction, which leads to enhanced catalytic activities, also leads to instability, and we address deactivation via sintering and strategies for its possible prevention. Lastly, we discuss selectivity and resistance to poisoning, properties that are also dependent on size and composition. Although examples of different systems are provided in this review, platinum clusters are used as a guiding thread. We refer to both experimental and theoretical findings. However, in view of our own expertise and contributions to the field, we capitalize on the role of and progress in realistic theoretical modeling. This type of modeling is critical for providing insight at the atomistic and electronic levels, as there the properties of clusters are dramatically altered by relevant conditions and the behavior of clusters becomes highly dynamical (fluxional). Therefore, in vacuo calculations of singular cluster structures or singular reaction events bring limited information. Instead, the field is in need of a holistic dynamical and statistical view on such catalytic systems, provided in conjunction with high-quality electronic structure treatments.

2. SIZE AND MORPHOLOGY EFFECTS

Small clusters of transition metals often exhibit unique catalytic activities. The oldest example, but still a striking one, is gold. Bulk gold is chemically inert and, in fact, it is the only metal that does not dissociatively chemisorb oxygen. Nevertheless, in 1987, Haruta et al. (42) found that Au nanoparticles were very effective catalysts. Now we know that Au nanoparticles with diameters below a few nanometers are catalytically active in a number of reactions (43, 44). In polydispersed nanocatalysts, even when most of the material is in the form of larger nanoparticles, nanoclusters are often (but not always) the true actors of catalysis. For example, in iron oxide–supported Au catalysts, the highest catalytic activity for carbon monoxide oxidation was found for nanoclusters of about 0.5 nm in size, i.e., containing about 10 Au atoms (45). Similarly, $Au_{6–10}$ clusters were pinpointed as highly active and selective for propylene epoxidation (46). The improved catalytic properties of clusters can be translated into lower reaction temperatures and energetic savings (47).

It is in the size regime of subnanoclusters, namely, nanoparticles of less than about 30 atoms, that one finds the greatest effect of cluster size. Here every atom counts (48). This means that catalytic properties can potentially be tuned through minor changes in size and/or composition. Size-dependent properties have been extensively studied for Pt nanoclusters in various reactions. The study of hydrogenation of ethylene on size-selected Pt_n ($n = 8–15$) soft-landed on MgO made it clear that the properties of nanoclusters cannot be simply extrapolated from properties at larger sizes (49). (De)hydrogenation reactions are structure insensitive for bulk platinum (49, 50); i.e., the turnover frequency does not change on different crystal planes of platinum. In contrast, MgO-supported Pt nanoclusters exhibit characteristics consistent with structure sensitivity. Unique reactivity was also revealed, since clusters containing more than 10 atoms were so reactive that the hydrogenation of ethylene started at 150 K. Among these Pt clusters, Pt_{13} was the most active.

When supported on alumina/tin oxide, $Pt_{8–10}$ clusters were observed to be superb catalysts in the oxidative dehydrogenation of propane (51). These small clusters were as selective as previously reported platinum or vanadia catalysts, but were 40–100 times more active. Density functional theory (DFT) calculations showed that this impressive reactivity in C–H bond activation, as compared to extended surfaces, resulted from the undercoordinative nature of Pt atoms in the nanoclusters.

The structural transition from two-dimensional (2D) to three-dimensional (3D) clusters also leads to completely different activities and selectivities, although there is no general or simple way to predict how catalytic properties will be affected. For Pt_n/rutile TiO_2(110), scanning tunneling microscopy showed a structural transition from 2D to 3D at $n = 8$, and this transition goes together

with a decrease in the activation energy for CO oxidation (52). Similarly, 2D and 3D $Pt_{4,6,8}$ clusters supported on anatase TiO_2(101) were compared using DFT (53, 54). 3D clusters were more active in the formation of bent CO_2^-, the key activated species in the CO_2 photoreduction reaction. The reason is that CO_2 adsorbs more strongly at the interface edge sites, and 3D structures provide a greater number of such sites. Moreover, 3D structures are more flexible (fluxional) and show large geometrical changes upon adsorption of CO_2. As a consequence, the orbital overlap between the cluster and CO_2 is maximized, achieving strong bonding, whereas 2D geometries are tightly bonded to the surface and exhibit very limited reconstruction. In contrast, alkene activation for dehydrogenation happens more readily on quasi-2D geometries of Pt_7/Al_2O_3, whereas the 3D isomers are catalytically irrelevant (55). Therefore, not only the size but also the morphology governs the properties of the nanoclusters, and the morphological influence is additionally dependent on the catalyzed reaction. These examples illustrate that the relation between size and catalytic activity is very complex and that different factors, such as temperature and the nature of the support and of the adsorbed reagents in the particular reaction to be catalyzed, have a great effect.

3. ENSEMBLE REPRESENTATION AND ENSEMBLE-AVERAGE PROPERTIES OF CLUSTER CATALYSTS

The information presented so far may inspire the overly simplistic, long prevalent view that cluster catalysts are rather stationary entities with well-defined and countable sets of possible binding sites. However, recent work has started to reveal the dynamic, statistical ensemble nature of cluster catalysts (56, 57), and theory has played a major role in this revelation.

Metal clusters are fluxional; i.e., they easily change shape as a result of the surrounding conditions or thermally as a result of the delocalized, nondirectional chemical bonds they contain, which lead to a wealth of potential energy surfaces of clusters in local minima of similar energies. This has two important consequences. On the one hand, different isomers might be populated at catalytically relevant conditions, offering many possible binding sites of very different coordinations. On the other hand, the relative stability of accessible cluster isomers and the probability for them to be populated might vary significantly with subtle changes in the environment, making their characterization challenging. Consider a simple example of the Pt_{13} cluster in the gas phase (**Figure 1**). The global minimum of this cluster is not a closed polyhedron that one can cut out of bulk platinum, but a less symmetric structure. However, through sampling of the configurational space, many other low-lying local minima are recovered, in close energetic proximity to the global minimum (56). Temperatures in catalysis can be high. In reactions of dehydrogenation typically catalyzed by platinum, the temperature is 600–700 K. If thermal fluctuations in the system are sufficient to surmount the barriers to cluster isomerization, Boltzmann statistics can be applied to obtain population percentages of all accessible minima. Entropic effects can be accounted for. Averaging over the ensemble would then produce experimentally observable properties, such as, for example, ensemble-average vertical ionization potential (VIP). In **Figure 1**, we show how the average first VIP varies as a function of temperature, i.e., as the number of isomers and the entropies grow. At high temperatures, this quantity is very different from that characteristic of the global minimum; also, whereas for Pt_{13} the VIP slowly grows, for Pt_9 it drops instead. In catalysis, conditions include other factors besides temperature, which further complicates the picture.

The size-specific catalytic activity of subnanocluster catalysts is therefore an ensemble-average property. Some accessible higher-energy isomers, though less populated, could be the most active. It is thus fundamental to take them into account. Cluster structural diversity and dynamic fluxionality are important features to capture in order to properly elucidate reaction mechanisms and gain insight essential for future design.

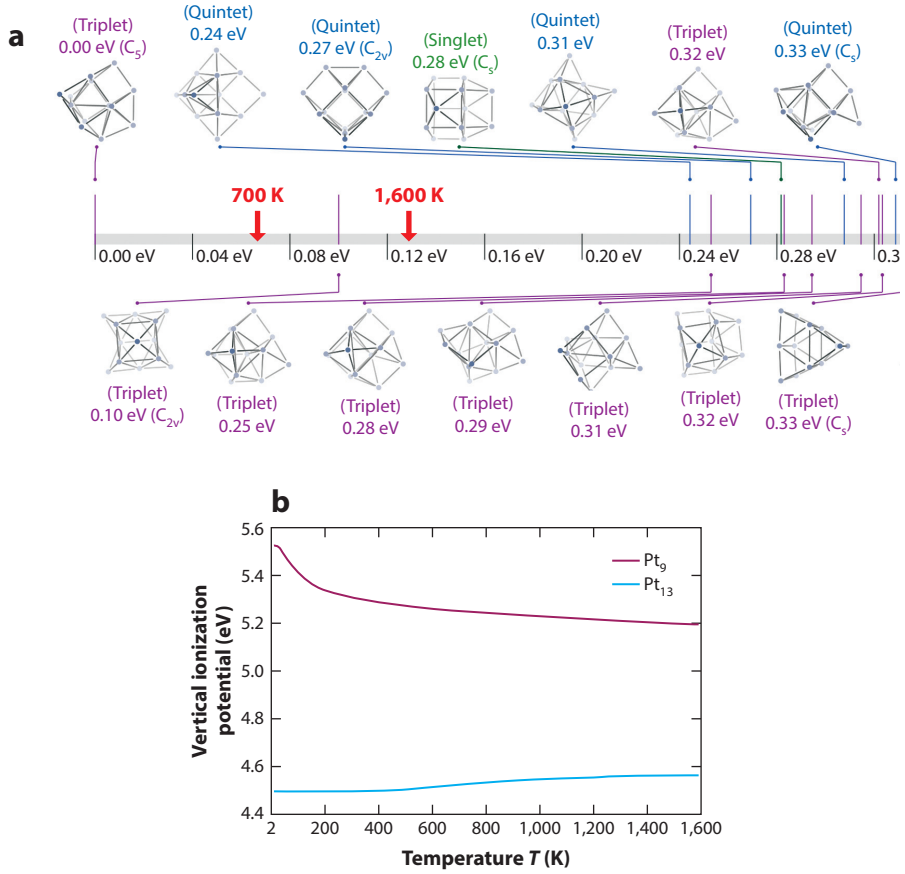

Figure 1

(*a*) The spectrum of low-lying isomers of Pt_{13} in the gas phase. (*b*) The ensemble-averaged first vertical ionization potential of Pt_{13} and of Pt_9 as a function of temperature, i.e., with inclusion of more isomers in the population and accounting for entropic effects as temperature increases. Figure adapted from Reference 56 with permission. Copyright 2016 American Chemical Society.

Advances have been made, both in multiscale modeling theory and in multimodal operando experimental characterizations, toward capturing some of the described realistic aspects of subnanoscale catalysis. From the computational standpoint, one difficulty is in the determination of the geometries of the catalyst, since shapes and overall potential energy landscapes of subnanoclusters are generally unpredictable. The search for relevant structures is now largely automated, and several algorithms have been developed for this purpose, including genetic (58–63), simulated annealing (64), particle swarm optimization (65, 66), and basin hopping (BH) (67) algorithms. Often, these methods rely on DFT for local geometry optimizations. However, even DFT is expensive in view of the required amount of sampling. To alleviate the computational cost of searching for global minima, classical force fields or neural network–based approaches have been applied to perform a preoptimization of every new geometry before handing it to DFT (56, 68, 69). Most of these methods are designed for gas-phase clusters, and thus one usually has to deposit the most stable cluster(s) with different orientations on different binding sites of the support in order to approximate the configurational space. Within this procedure, one may easily remain

trapped in metastable high-energy minima. Fortunately, some of these algorithms are adapted for surface-deposited clusters (70, 71).

The importance of higher-energy structures of supported size-selected nanoclusters for catalysis was only recently realized (55, 56, 72–74). The example of ethylene dehydrogenation on Pt_7 and Pt_8 on Al_2O_3 illustrates the relevance of ensemble representation (55). Experiments show that Pt_7 supported on Al_2O_3 is significantly more active toward dehydrogenation of ethylene than Pt_8 and Pt_4, which exhibit comparable activities. The global minima of supported Pt_7 and Pt_8 give no answer to this puzzle, since both have 3D geometries with comparable properties. However, meaningful differences arise when considering not only the most stable isomer, but all the isomers that are predicted to be populated at the catalytic temperature of 700 K. As shown in **Figure 2**, all the relevant Pt_8 conformers have 3D morphologies, and the global minimum is highly dominant in the population ($P_{700\,K} = 87.7\%$) according to Boltzmann statistics. By contrast, Pt_7 has significant thermal access to 2D isomers that become more and more predominant upon increasing temperature. These 2D structures feature greater charge transfer from the support and more binding sites that can activate ethylene for dehydrogenation rather than for hydrogenation or desorption. Differences in accessible structures were confirmed through ion scattering experiments and through CO temperature-programmed desorption (TPD) that assessed the number of exposed Pt binding sites at catalytically relevant temperatures (55). Size-specific activity was attributed to this morphological difference in the Pt_7 and Pt_8 ensembles.

In a more general sense, the nature of the available binding sites in the ensemble of clusters can be used to make first estimations of properties. As we see in the example above, Pt_7 offers a wider variety of binding sites for adsorbates as opposed to the more uniform structural isomers of Pt_8. Every site is characterized by its own coordination environment; electronic structure; and, therefore, affinity to reagents, such as ethylene, coke, or products of partial dehydrogenation. Hence, structural diversity leads to the availability of sites, some of which may have the desired optimal affinity for the rate-determining intermediate, i.e., would place the given site at the tip of the Sabatier volcano. The effective catalytic activity of the ensemble, therefore, depends on the activity of every available site on every accessible cluster structure, weighted by the availability of this structure in the population. This statistical definition of size-specific activity of cluster catalysts is very different from the more traditional, stationary, single-cluster view. The worst-case scenario would be if the diversity of sites were so vast that the population exhibited detectable activity toward all processes, since any incoming species would be able to find the binding site with just the right affinity. Selectivity, as well as deactivation by poisoning agents in such conditions, could be a problem. Note, however, that the selectivity aspect of cluster catalysis presented in this way is yet unexplored. Obviously, the preferred scenario is when the sites that are most active toward desired processes are also highly abundant, but even a low concentration of very special active sites can make a good catalyst. It can help if sites of undesired selectivity are permanently occupied by adsorbates.

4. EFFECT OF COVERAGE

It is noteworthy that the structures and relative stabilities (i.e., availability in the population) of all the minima depend heavily not only on temperature, but also on the support and on the chemical nature and coverage of adsorbates, such as reactants, reaction intermediates, and poisoning agents. We discuss coverage first and address the effect of the support below. The adsorbates can radically change the energy landscape of a nanocluster. This was beautifully illustrated in a study of H adsorption on the Pt_{13} cluster supported on γ-alumina (75). In the absence of hydrogen, the ground state of Pt_{13} was predicted to be biplanar, allowing it to maximize its interaction with the

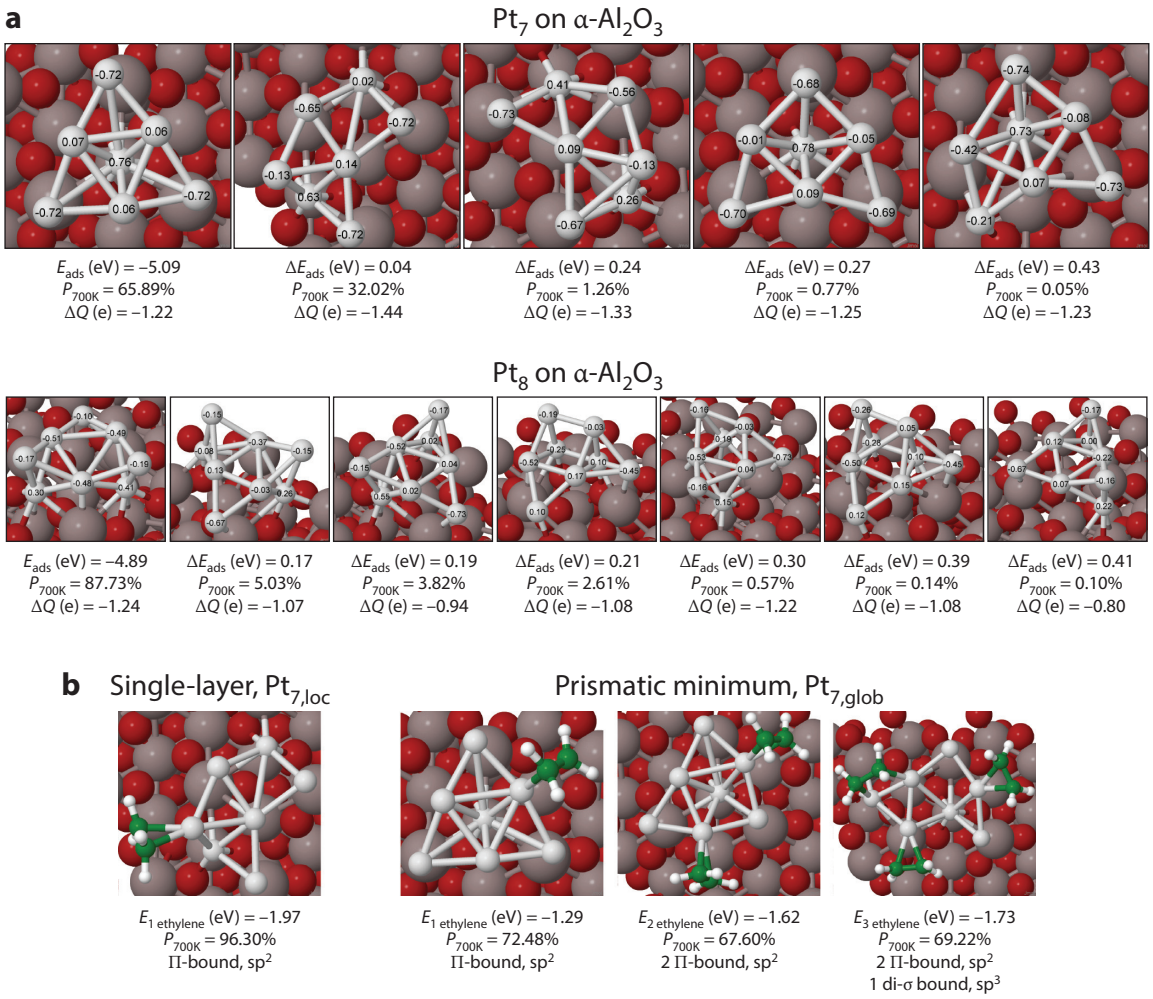

Figure 2

(*a*) Lowest-energy minima of adsorbed Pt_7 and Pt_8 with adsorption energies (E_{ads}), Boltzmann population at 700 K ($P_{700\,K}$), and charge transfer from the support to the clusters (ΔQ). (*b*) Examples of structures obtained for Pt_7/Al_2O_3 with adsorbed ethylene, with ethylene adsorption energies, prevalence in the population at 700 K, and the bonding character in the adsorbed ethylene shown. Upon the adsorption of one ethylene molecule, the second, single-layer isomer becomes more stable than the prismatic one that used to be the global minimum in the absence of adsorbates. By the time three ethylene molecules are adsorbed, the prismatic structure spontaneously undergoes isomerization to the single-layer one. Figure adapted from Reference 55.

surface. A high degree of hydrogen coverage (H/Pt > 1.4), however, induces a reconstruction from biplanar to cuboctahedral morphology because of the greater ability of the latter to adsorb hydrogen. Hence, the very nature of the catalyst is adsorbate dependent. Catalyst structure and catalyzed reaction are mutually dependent. This example shows the need to perform global catalyst structure searches in the presence of adsorbates.

This statement applies even to such relatively simple events as reverse spillover from the support to the cluster. For Pt_6 on $CeO_2(111)$, the global minimum structure (**Figure 3*a***) was

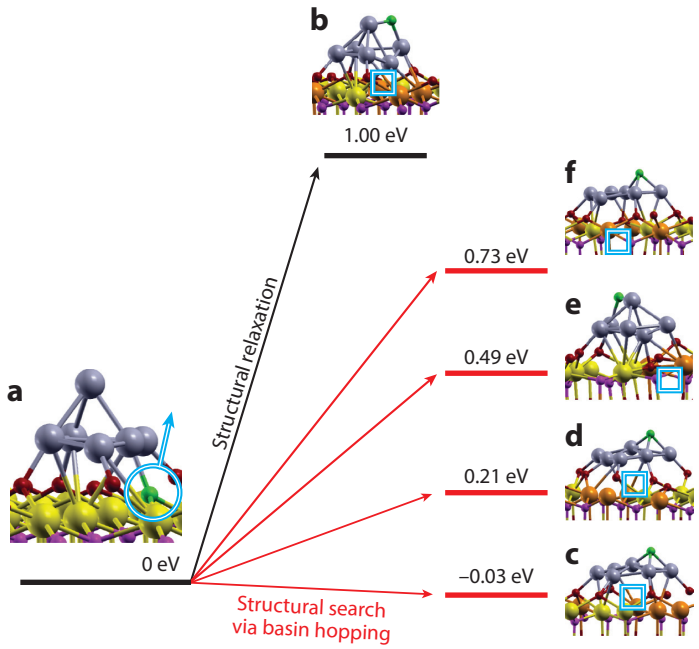

Figure 3

(*a*) The global minimum of Pt_6/CeO_2; the green O atom is the candidate for reverse spillover from the cluster–surface interface. (*b*) The most stable isomer after reverse spillover starting from the structure in panel *a*. (*c–f*) The most stable isomers after reverse spillover identified using a basin hopping search. Figure adapted from Reference 76 with permission. Copyright 2014 American Chemical Society.

found using the BH algorithm (76), and then two computational approaches were applied to study the reverse oxygen spillover. This process consists of the formation of an O vacancy at the platinum–support interface and the migration of that O atom to the cluster. In the first approach, the final state, i.e., that in which the O atom had already migrated to the cluster, was obtained by a local geometry optimization for each possibility of moving an interfacial O atom, starting from the global minimum of Pt_6/CeO_2. The most stable structure obtained in this way is depicted in **Figure 3*b***. In the second approach, a BH optimization of the final state was performed, and several structures significantly more stable than this (by almost 1 eV) were found (**Figure 3*c–f***). There is no resemblance of the BH-identified most stable isomer with the initial structure of Pt_6 on CeO_2. In practice, which one of the isomers would actually form in catalysis depends additionally on the kinetics. But this example illustrates that it is unsafe to assume minimal rearrangements of the cluster catalyst and to trust that large barriers would keep it fixed. Taking this one step further, we can infer that the catalysts' potential energy surfaces change when transitioning from reactants to intermediates to products. In the language of a statistical ensemble, we should say that the ensemble changes, not the single structure.

In Baxter and colleagues' (55) study on size-selected Pt clusters supported on alumina for ethylene dehydrogenation, accounting for ethylene coverage was essential to capturing the role of the second-lowest energy minimum of Pt_7/Al_2O_3 rather than the global minimum (**Figure 2*b***). Whereas in vacuo the prismatic isomer is the global minimum, as soon as a single ethylene molecule adsorbs, the order of the isomers reverts and the single-layer isomer becomes more stable. Since the single-layer isomer pulls more negative charge from the support, it is more nucleophilic and binds ethylene more strongly, bringing the overall energy of the system below

the former global minimum. Ethylene TPD experiments showed that the cluster can adsorb up to three ethylene molecules, and therefore the computational work was extended to this relevant coverage. By the time three ethylene molecules are adsorbed, the prismatic isomer undergoes a barrierless isomerization toward the single-layer configuration. It was thus demonstrated that the single-layer isomers are the real players in catalysis. This work emphasizes the additional important point that, in realistic conditions, key active sites may emerge that are metastable or not present in ambient conditions, i.e., before the catalyst is brought to its activated state. Therefore, in order to identify the catalytically relevant sites and truly understand reaction mechanisms, operando characterization techniques and a tour de force of realistic modeling are required.

Bridging the pressure gap (i.e., the pressure difference in surface-science modeling experiments versus in real catalysis) requires accounting for pressure effects on the underlying support. In this regard, an important consideration for oxide surfaces is the presence of hydroxyl groups (77). The hydroxylation state of an oxide is a complex matter that depends on several factors, such as the type of oxide, the surface orientation, and the chemical potentials of oxygen and water (78). Hydroxyl groups are known to play a role in catalytic reactions, either by modifying the electronic properties of the catalyst or by participating in the reaction (79, 80). Similarly, the shape and sintering behavior of nanoparticles depend on the hydroxylation level of the underlying oxide, although this relation may not be straightforward (81). Other surface species also influence clusters. Chlorination, for instance, helps to mitigate the sintering of Pt nanoclusters supported on γ-alumina (82, 83). Therefore, it is important to include such species in simulations.

5. ELECTRONIC METAL–SUPPORT INTERACTION

In catalysis, metallic nanoclusters are usually dispersed on oxide supports with high surface area. For small clusters, most of the cluster atoms are at the interface with the support, which greatly impacts the chemical properties of the cluster. Campbell (84) called this phenomenon electronic metal–support interaction (EMSI). The support plays a crucial role in modulating the geometric and electronic structure of the nanocluster and, thus, its catalytic properties, as well as its stability against sintering (78, 85, 86). EMSI may be weak (van der Waals interaction) or strong (covalent and/or electrostatic interaction). The extreme form of EMSI is strong metal–support interaction (SMSI). SMSI was initially considered to be harmful to the catalyst because of the formation of an oxide layer on the surface of the metal nanoparticle (87, 88). By now, several works have demonstrated that SMSI can substantially enhance the catalytic properties of metal nanoparticles (89–91). Interaction with the support adds a level of complexity to the system, but also another degree of freedom to achieve the greatest performance of the catalyst and stability against deactivation.

The electronic structure of the nanocluster is affected by charge transfer between the catalyst and the support. The direction and amount of the charge transfer can, in principle, be tuned by the nature of the oxide, defects, doping, etc. Nonreducible oxides, such as MgO, CaO, and Al_2O_3, are characterized by large band gaps and low reactivity. The charge transfer at the interface is usually small. Defects can turn charge transfer and can also be fully responsible for catalyst activation, as is the case for Au_8 in CO oxidation, which is active only when deposited on a MgO surface containing O vacancies (F-centers) because of increased charge transfer from the support to the catalyst (92). For $Au_{15}Cu_{15}$ supported on MgO, F-centers again facilitate CO oxidation, whereas Mg vacancies (V-centers) reduce the charge transfer to the cluster and harm the activity. However, the V-centers provide the strongest binding to the surface, making sintering less likely (93).

In reducible oxides, such as TiO_2 and CeO_2, the metal has access to several oxidation states, so its oxidation state can easily be lowered. The bond between the metal and oxygen has a less pronounced ionic character and, unlike in nonreducible oxides, the oxygen still has oxidizing power

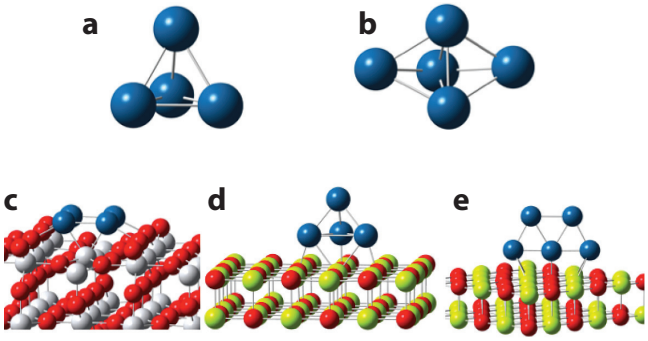

Figure 4

The most stable isomers of (*a*) Pt_4 in the gas phase, (*b*) Pt_5 in the gas phase, (*c*) Pt_4 on TiO_2(110), (*d*) Pt_4 on MgO(100), and (*e*) Pt_5 on MgO(100). Deposition on a substrate can alter nanocluster morphology in potentially surprising ways, as can be seen by comparing panels *a*, *c*, and *d* and comparing panels *b* and *e*. Data from References 97, 98.

(78). Consequently, these surfaces can easily accept charge from a donor species. The occurrence and direction of charge transfer can be optimized by controlling the thickness of the oxide film (94) or by the inclusion of defects or dopant atoms. For instance, on TiO_2 anatase and tetragonal ZrO_2(101) doped with nitrogen, Ag and Au clusters become positively charged (95). As a result, the cluster–support interaction is enhanced, since both the surface and subsurface nitrogen dopant anchor the cluster to the surface.

The substrate can have a marked effect on the morphology of the cluster, which, again, is important for catalytic properties in structure-sensitive reactions. For Au_mRh_n ($4 \leq m + n \leq 6$) (96), for example, interaction with MgO can change a 2D structure to a 3D structure (or vice versa) upon deposition. The reason is that the interaction of the substrate with Rh atoms is more favorable than with Au atoms. We are learning the logic behind shape transformations, but the relative weights of all the factors governing shape transformations, such as the strength of atom–support interactions versus the strength of intracluster bonding for a given shape and composition, are not trivial to predict, although they can be computed. Hence, the way in which the support alters the morphology of the cluster can be surprising, as shown in **Figure 4**: Gas-phase Pt_5 is a trigonal bipyramid, but upon deposition on MgO it becomes planar and stands upright as a result of charge transfer, induced partial covalency, and repulsion with the negatively charged O atoms at the surface (97). Pt_4 in the gas phase also has a 3D structure, and upon deposition on MgO, its structure remains approximately the same. This more compact shape results from the slight dominance of intracluster bonding over coordination to the support. The situation is completely different when this cluster is supported on TiO_2(110): Pt_4 adopts a square-planar shape, which provides increased interaction with this support (97, 98). Of course, we have so far discussed only ground-state geometries, but the entire ensembles show marked differences when going from the gas phase to the surface (e.g., 26, 28, 99).

Overall, cluster–support interaction can be a powerful tool for tailoring and optimizing the properties of catalysts. A beautiful example is Au_{20}. In the gas phase, the ground state of Au_{20} is a pyramidal structure with a very high HOMO–LUMO gap of 1.77 eV (100). This cluster has very limited reactivity and is not useful for catalysis (101). However, the Au_{20} cluster can also adopt a 2D planar structure. This conformer is thermodynamically less stable but catalytically more active. When deposited on MgO or graphene, the 3D isomer is still the most stable one. In light of this situation, various ways of stabilizing the catalytically active isomer by tinkering with

the substrate have been proposed. One idea is to use an ultrathin layer of MgO on an underlying metal surface of Mo(100) as support (102–104). Another way of stabilizing the planar isomer is by doping the surface, e.g., doping MgO with aluminum (105) or doping graphene with nitrogen (106). Other proposed ideas include growing the system (cluster and MgO support) in the presence of an electric field (107) and depositing Au_{20} on pristine silicene/Au(111), allowing strong Si–Au covalent bonds (108). In all cases, the morphological transformation is caused by a substantial charge transfer from the support to the cluster. As a result, the excess charge on the supported 2D Au_{20} conformer makes it an even better catalytic agent for the oxidation reaction of CO.

We emphasize that it is extremely difficult to predict how a specific metal–support interaction will affect the chemical properties of a catalyst. For example, Co nanoclusters were deposited on different oxide supports (MgO and Al_2O_3) and on an inert carbon-based support [ultrananocrystalline diamond (UNCD)] for use in the Fischer–Tropsch synthesis (109). The overall activity was greatest in the case of UNCD support. Moreover, this system exhibited the highest selectivity toward the formation of longer-chain hydrocarbons. This effect was correlated to the oxidation state of the metal. Similar studies were performed for Ag clusters catalyzing the epoxidation of propylene (110). In this case, however, it was found that whereas Ag nanoclusters are highly efficient catalysts when supported on alumina, they become inactive when deposited on UNCD. It was proposed that the lack of metal-oxide interfacial sites in the case of Ag on a UNCD support limits the epoxidation catalytic activity. This result points out the extreme effects of interaction between the support and the metal catalysts, opening a wide range of possibilities to optimize specific catalytic processes.

One more pending matter in terms of realistic modeling is the transition from crystalline surface models to amorphous supports, which are relevant in industry. A recent work pointed to the need of modeling such supports after comparing Pt_{10} on highly ordered alumina (obtained under UHV conditions) and Pt_{10} on an amorphous alumina substrate (111). Interestingly, the authors found that, when exposed to realistic reaction conditions, Pt_{10} on ordered alumina undergoes a morphological transition to a system very similar to Pt_{10} on amorphous alumina. The computational modeling of amorphous supports is difficult because of the diversity of surface features, the need for a bigger unit cell, and limited experimental data. The approach to modeling amorphous supports that has so far been most successful is based on classical molecular dynamics (MD) refined with density functional theory (DFT) (112–114). Some theoretical studies of amorphous surfaces as supports for nanoclusters have been successful, with results comparable to experimental data (115, 116), but more research in this direction is definitely needed.

6. CLUSTER CATALYST STABILITY

The interaction between the metallic clusters and the underlying surface is furthermore intimately linked to the longevity of the catalyst. Indeed, a major challenge in achieving routine use of metallic nanoclusters as catalysts is their instability against deactivation via poisoning and sintering, or thermal agglomeration into large particles aiming to reduce the surface energy. Whereas poisoning is reaction-specific, sintering is universal to most subnanoclusters, especially in catalytic processes that require high temperatures, such as steam reforming. Sintering causes the loss of active sites and size-specific catalytic characteristics. Thus, the stabilization of nanoclusters against sintering is fundamental for their applications.

Sintering can happen via two major mechanisms: Ostwald ripening (OR) and cluster coalescence, or Smoluchowski ripening (SR). In the OR regime, an atom leaves the cluster and migrates through diffusion, either on the surface or through the vapor phase, in order to join larger particles. The SR regime involves Brownian motion of entire nanoparticles on the support, leading to

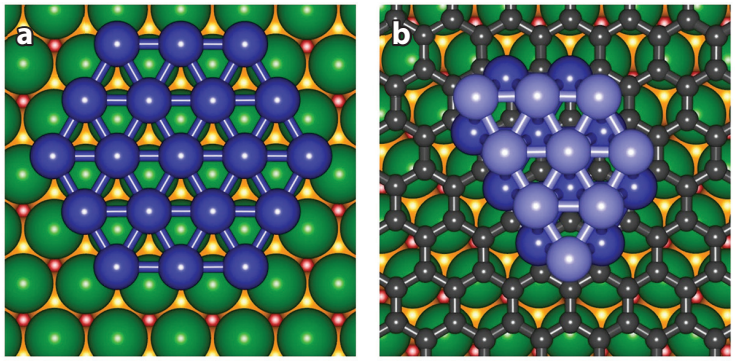

Figure 5

Pd_{19} supported on (*a*) Rh(111) and (*b*) a graphene moiré film on Rh(111). Figure adapted from Reference 123 with permission.

their coalescence and agglomeration. When particles are very small (a few atoms), the mechanism of sintering has been more often (117–120) than not (121) observed to be the OR mechanism.

In general, the mechanism depends on the relative strengths of intracluster bonding versus cluster–support bonding, as well as on some additional entropic factors. In fact, the ripening modes can be changed between OR and SR by tuning the interactions with the substrate (122, 123). This was evidenced when Pd clusters were deposited on particular substrates and the ripening regimes compared (123). On Rh(111) (**Figure 5*a***) and on hexagonal BN moiré films on Rh(111), Pd clusters sinter via OR. In contrast, on graphene moiré films grown either on Rh(111) or on Ru(0001) (**Figure 5*b***), the binding energy to the support is weaker, and Pd clusters coarsen by the SR mechanism. On these supports, OR can be observed only at very high temperatures. Stronger cluster–support interactions discourage SR. For example, Ag clusters sinter with markedly different speeds on ceria and magnesia (124). To control sintering, functionalization of the support and introduction of dopants are being explored with some success (125–127). Oxidized Co_4 clusters were found to be resistant to sintering whenever they were supported on alumina or on UNCD (128), but the reasons for the stability were different for each support. Alumina anchors the clusters through bonds between Co and surface O and between cluster O and aluminum. On UNCD, the origin of the sintering resistance lies in electrostatic and dispersive interactions at the hydrogen-terminated pristine surfaces, as well as in covalent bonds between the cluster and the defect sites of the support. We note, finally, that changing the cluster–support interaction will also affect the activity. Hence, activity and sintering resistance should ideally be optimized simultaneously.

An alternative way to discourage SR is by preventing the fusion of clusters upon coalescence. A pioneering work achieved a sintering-resistant Ir catalyst supported on MgO in this way (122). This so-called "smart" catalyst consists of clusters of a critical size (nearly 1 nm, or about 40 Ir atoms) that do not fuse, even if they collide with other clusters, because they possess rigid cubic structures and the energy penalty to rearrange the atoms to merge is too high. The effect was not repeatable for Pt and Au, however.

OR, by contrast, can be mitigated by increasing the strength of intracluster bonding, for example by nanoalloying with other elements. Pt nanoclusters deposited on MgO, for instance, are predicted to be more OR-resistant if doped with boron (72, 129): Covalent Pt–B bonds distort and stabilize the clusters, increasing the barrier to Pt atom dissociation and thus reducing the propensity to sinter. Another, and perhaps the most successful, approach to reducing OR is based on the idea that the driving force for OR is provided by the different chemical potentials of

particles with different sizes. If all the particles have the same size, OR might be suppressed. This has been shown for Pt clusters on different supports (130). Thus, a perfectly monomodal initial size distribution is an attractive solution for fighting OR.

Other methods of preventing sintering have to do with the architecture of the support physically preventing clusters from disassembling and migrating, and include the use of isolated pores, or pits on the surface, as well as overcoating after cluster deposition. We do not discuss these techniques here, as our focus is on clusters.

Our understanding of the process of sintering comes largely from microscopy (28, 41). To theoretically probe the process, multiscale ensemble simulations mimicking the effect of temperature are required. For example, to explain the phenomenon that alloying Pt with an equal amount of Pd reduces sintering of the clusters on oxides (131), which had been observed experimentally but not yet understood, a Monte Carlo (MC) scheme was devised (132) (**Figure 6**). First, the global minimum and all thermally accessible local minima of Pt_xPd_{n-x} ($n = 4$–0, $x = 0$–4) deposited on TiO_2 were found using DFT. The energy of the cluster of every stoichiometry was then taken as an ensemble average over the structures that exist at the temperature of interest as defined by Boltzmann statistics (this was the first way to account for temperature, T). All atom-dissociation energies were also precomputed. Finally, the full potential energy surfaces for the single Pt and Pd atoms on TiO_2 were computed. The simulations began with tossing of Pt and Pd atoms onto the support at the desired coverage. Allowed MC moves included atom jumps from site to site over a fine grid on the support, association to form clusters with precomputed energy gains, and dissociation from clusters with precomputed penalties. All energy components went into the MC acceptance criterion, which also contained T. Simulations reproduced the experimentally known fact that clusters with Pt:Pd = 1:1 survive the most during sintering. The main reason for the stability was identified to be entropic: Since such clusters have considerably more thermally accessible isomers than do clusters with other Pt:Pd proportions, configurational entropy contributes to the free energy of the system in a favorable way.

The algorithm was later extended to allow for atom evaporation and redeposition to account for atom loss and possible OR via the vapor phase (98). The extended algorithm showed that PtZn clusters on MgO(100) and TiO_2(110) sinter rapidly, but in different ways. Zn easily evaporates from magnesia, but binds strongly to Ti atoms on titania. This results in Pt-rich sintered phases on MgO and in separate Pt-rich and Zn-rich sintered phases on TiO_2 (98). These simulations still do not consider the effects of adsorbates.

The shortcoming of these sintering simulations is the lack of adsorbates, which would necessarily be present in reaction conditions and could influence the stability of the clusters (133, 134). In fact, high pressures of H_2 and O_2 can enhance the sintering of metallic nanoclusters (135–137). Bound CO weakens and distorts deposited Au clusters and should therefore accelerate sintering. The atomistic information that simulations provide is crucial for eventual mitigation of sintering, and therefore algorithmic capabilities should develop in this direction.

7. ROLE OF CLUSTER FLUXIONALITY IN REACTION DYNAMICS—THE LATEST FRONTIER

Notice that so far, modeling accounts for the statistical distributions of shapes in the ensemble at a given temperature. An added degree of complexity comes from the dynamics. The fluxional nature of clusters (57, 138, 139), of course, contributes to the thermal rearrangements in the ensemble, in the minima on the free energy surface, e.g., in the well of the reactants or intermediates of the catalyzed reaction. Some isomers that we discover and include can be kinetically trapped or unreachable, and it is therefore important to balance the populations by the kinetic effects.

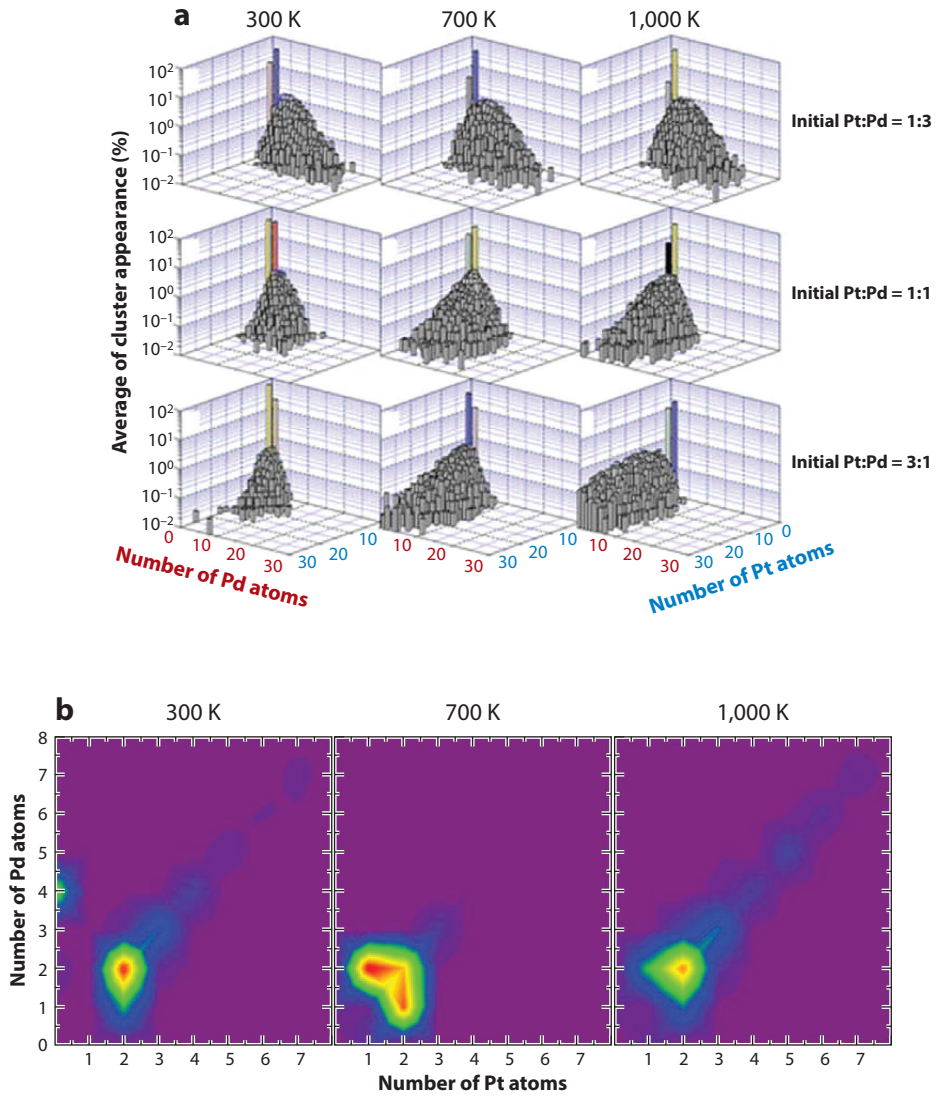

Figure 6

(*a*) Sintering simulation of mixed PtPd clusters with different initial Pt:Pd ratios and different temperatures: All conditions favor the retention of clusters that consist of equal numbers of Pt and Pd. (*b*) The middle row of panel *a* viewed as a heat map, i.e., from above, showing cluster buildup around the diagonal where the numbers of Pt and Pd atoms are equal. Figure adapted from Reference 132 with permission. Copyright 2014 American Chemical Society.

Born–Oppenheimer MD reveals that Au12 and Au13 gas-phase clusters, for example, exhibit different topologies that cyclically interconvert at room temperature, being highly fluxional. In contrast, Au20 is not as fluxional and shows high stability in its pyramidal shape (140). Clearly, the support will play an important role in a cluster's fluxionality, facilitating or hindering certain morphologies (141). Theoretically approaching these effects is not simple. A limited picture

can be given by MD, although it would recover only a fraction of viable pathways. A fuller thermodynamics–kinetics map of cluster catalysts would be highly desirable.

Nevertheless, even more formidable is the possibility that cluster fluxionality can couple to the reaction coordinate. Notice that this is different from isomerization and re-equilibration of the cluster ensemble before or after the reaction step. It is much harder to capture, and may have dramatic consequences for the calculated reaction rate. In some cases, clusters undergo a small flexing or adaptation of structure as part of the reaction event in order to provide the most favorable reaction path (55, 142). Indeed, this behavior can be one of the keys to success in cluster catalysis. Yang et al. (53) defined a displacement to describe the extent of the structural flexibility of a cluster using the following formula:

$$\text{Displacement} = \sum_{n} \frac{\sqrt{(X_{nf} - X_{ni})^2 + (Y_{nf} - Y_{ni})^2 + (Z_{nf} - Z_{ni})^2}}{M}, \qquad 1.$$

where X, Y, and Z represent the coordinate of the n-th atom in the cluster, i and f represent the initial and final states, and $n = 1 - M$, with M being the number of atoms of the cluster. This formula was applied to compare the two main isomers of Au_{13}, icosahedral and cuboctahedral (143). In the gas phase, the cuboctahedral conformer is more stable, but when deposited on partially reduced anatase TiO_2(101), the icosahedral cluster becomes more stable after a significant reconstruction. The latter isomer binds CO_2 more strongly after altering its structure; it can easily adopt different configurations to optimize CO_2 adsorption. When the above formula was applied, it was shown that there is a direct relation between the higher displacement of the icosahedral cluster and a larger CO_2 adsorption energy. Thus, a more flexible isomer is able to adapt to the environment, increasing its interaction with the substrate as well as facilitating its binding to the reactants. This type of flexing is not problematic for theory. True cluster isomerization, however, is more dramatic and involves crossing a barrier. The question is, can this kind of isomerization happen simultaneously with the reaction step, and lower its barrier, in a coupled reaction path (57)? It is not inconceivable, considering the nondirectional bonding in metallic clusters. This might be system dependent, and not something that has a universal answer or approach for capturing, as happen so often with nanocatalysts. Computational modeling will be vital to clarifying this question because it allows, in principle, a separation of the diverse components of a given system. There is much work to do in this respect, and new theoretical strategies and algorithms must be developed.

8. COMPUTATIONAL METHODS

There are two major avenues in the computational methodologies that, in our view, require algorithmic developments: the statistical mechanical and quantum mechanical avenues. To computationally study nanocatalysis, one would ideally use global optimization sampling to determine the structures that will be populated under catalytic conditions and, eventually, calculate the reaction mechanism. As described in this review, this task can be extremely complicated. Catalytic conditions imply high temperatures and coverage with adsorbates, which will simultaneously influence both the support (e.g., contribute to the creation of defects) and the metallic nanoclusters (via fluxionality and induced restructuring). The structure on the interface will in turn affect the coverage. Hence, not only is the problem massive, but it also needs to be solved self-consistently. For simulations to be feasible, simplified models are needed, such that adequate computational methods that are still sufficiently accurate can be used (144). Smart sampling and global optimization strategies are being developed to reduce the computational cost as much as possible.

Generation of ensemble descriptions of cluster catalysts in realistic conditions needs to follow, but so far precedents of this sort are very rare.

Electronic structure offers another complication. Empirical potentials and force fields are popular and computationally inexpensive, but they are not accurate for transition metal clusters, and therefore more sophisticated (and expensive) methods must be used. DFT currently offers the best balance between accuracy and computational cost. The systems to study are large. Surface-deposited clusters are modeled as supercell slabs within periodic boundary conditions. The size of the supercell can become problematically large when dealing with bigger clusters (i.e., six or more atoms), to avoiding cluster–cluster interactions. The vacuum space between repeating images in the *z*-direction and the thickness of the slab also have to be large enough to avoid spurious surface–surface interactions. Nowadays, artificial electrostatic forces across the vacuum can be avoided using dipole corrections, which are implemented in most periodic code.

However, one needs to be careful when using DFT for surface-deposited clusters. The relative energies of cluster isomers often depend on the DFT method employed (56). Furthermore, for strongly correlated systems, DFT can produce completely unreliable results because of the lack of cancellation of the Coulomb self-interaction of an electron with itself and also because of the intrinsically single-reference nature of the method. This is the case for late transition metal clusters (e.g., clusters of Co and Ni and their oxides, often popular in catalysis), and rare earth oxide supports (e.g., ceria) (145). Many electronic states differing by electron localization or type of magnetic coupling of unpaired spins can be found close in energy in these systems, and the coupling between these states can be strong. As a result, the description should contain a superposition of multiple single-determinant states. More sophisticated electronic structure methods are then required for an even qualitatively correct description (146), and such methods for properly describing strongly correlated systems either are not yet implemented for periodic systems or are too expensive to use (as is the case for the random-phase approximation; see 147, 148). Hybrid functionals can help only to a limited extent, as they are still intrinsically single-reference. Additionally, it is not known a priori how much Fock exchange should be introduced in a hybrid functional for best agreement with experiment. A less computationally demanding (and therefore widely used) corrective scheme to treat these systems is the addition of the Hubbard *U* term to a set of atomic-like orbitals (e.g., to cerium f-states in the case of CeO_2) (149, 150). Although the *U* value can be chosen on a self-consistent basis (151, 152), it is most often chosen to fit a given property. Again, however, DFT+*U* does not capture static electron correlation. This means that DFT+*U* calculations address just one electronic state instead of a superposition, and even that state has broken symmetry. In addition, there is no guarantee that, if a given flavor of DFT predicts that the single chosen state is the lowest-energy one, the prediction is correct. In our opinion, the blind use of DFT+*U* is dangerous. It is too often abused, likely generating many results and predictions that will eventually prove wrong. A prime example of this is a large body of literature on ceria-supported cluster catalysts treated with DFT+*U*. Despite developments such as hybrid functionals based on a screened Coulomb potential (153) and methods using Green's function (154), the field is still in need of trustworthy electronic structure methodologies for strongly correlated systems.

9. CONCLUSIONS

With increasing environmental concerns worldwide, the use of nanoparticles as catalysts is a novel way to exploit resources more efficiently. Surface-deposited metallic nanoclusters have the potential to be superb catalysts, with unique and unexpected activities and selectivities. For practical applications, selectivity and cluster stability against sintering and poisoning need to be improved.

Cluster catalyst design is a balancing act, with multiple mutually entangled components needing to be simultaneously optimized. Catalyzed reactions are sensitive to clusters' geometric and electronic structures, and at the same time these structures are greatly affected by the nature of the adsorbates present and the temperature of the reaction. The support additionally influences cluster structure, stability, and properties, including catalytic activity, but stability and activity can be in contradiction. Structural diversity in the ensemble of cluster structures accessible under catalytic conditions is an important feature that often allows for the formation of otherwise metastable but catalytically relevant sites, or for clusters' dynamical adjustment to the reaction event, lowering the barrier. However, structural diversity and dynamic fluxionality may lead to the reduced selectivity of the catalytic process. Additionally, important metastable sites are difficult to identify and characterize under working conditions and are especially difficult to deliberately generate. In fact, it may be best to carry out the synthesis of a catalyst under the same conditions at which it will eventually operate. In terms of characterization, operando techniques should play a major role and should also use input from surface science. Theoretical modeling, in order to be useful, should fully depart from the paradigm of a single stationary structure and should include effects of temperature, coverage, and dynamics.

In view of this complexity, it is not surprising that cluster catalysts are not routinely amendable to design, and many discoveries in this field are still accidental. However, through modern and developing techniques, we start gaining understanding of how cluster catalysts operate and which factors are important for their special properties. Several modest but successful attempts at design or strategic modification have been reported. Therefore, we are optimistic about the future rise of strategic design and the precision synthesis of stable cluster catalysts with abundant catalytic sites of desired activity and selectivity.

DISCLOSURE STATEMENT

The authors are not aware of any affiliations, memberships, funding, or financial holdings that might be perceived as affecting the objectivity of this review.

ACKNOWLEDGMENTS

This work was supported by the Air Force Office of Scientific Research under a Basic Research Initiative grant (AFOSR FA9550–16–1–0141) and NSF CAREER Award (CHE-1351968) to A.N.A. E.J.-I. was supported by a Postdoctoral Fellowship of the Basque Country.

LITERATURE CITED

1. Spiewak BE, Cortright RD, Dumesic JA. 1997. Thermochemical characterization of heterogeneous catalysts. In *Handbook of Heterogeneous Catalysis*, ed. G Ertl, H Knözinger, J Weitkamp, pp. 698–706. Weinheim, Ger.: Wiley-VCH
2. Yu S-H, Tao F, Liu J. 2012. Editorial: Catalyst synthesis by design for the understanding of catalysis. *ChemCatChem*. 4:1445–47
3. Bell AT. 2003. The impact of nanoscience on heterogeneous catalysis. *Science* 299:1688–91
4. Roduner E. 2006. Size matters: why nanomaterials are different. *Chem. Soc. Rev.* 35:583–92
5. Lei Y, Mehmood F, Lee S, Greeley J, Lee B, et al. 2010. Increased silver activity for direct propylene epoxidation via subnanometer size effects. *Science* 328:224–28
6. Fu F, Xiang J, Cheng H, Cheng L, Chong H, et al. 2017. A robust and efficient Pd_3 cluster catalyst for the Suzuki reaction and its odd mechanism. *ACS Catal.* 7:1860–67

7. Guan H, Lin J, Qiao B, Yang X, Li L, et al. 2016. Catalytically active Rh sub-nano clusters on TiO_2 for CO oxidation at cryogenic temperatures. *Angew. Chem. Int. Ed.* 55:2820–24
8. Shimizu K, Sawabe K, Satsuma A. 2011. Unique catalytic features of Ag nanoclusters for selective NO_x reduction and green chemical reactions. *Catal. Sci. Technol.* 1:331–41
9. Concepción P, Boronat M, García-García S, Fernández E, Corma A. 2017. Enhanced stability of Cu clusters of low atomicity against oxidation. Effect on the catalytic redox process. *ACS Catal.* 7:3560–67
10. Kaden WE, Kunkel WA, Roberts FS, Kane M, Anderson SL. 2014. Thermal and adsorbate effects on the activity and morphology of size-selected Pd_n/TiO_2 model catalysts. *Surf. Sci.* 61:40–50
11. Pellin MJ, Riha SC, Tyo EC, Kwon G, Libera JA, et al. 2016. Water oxidation by size-selected Co_{27} clusters supported on Fe_2O_3. *ChemSusChem* 9:3005–11
12. Yang B, Liu C, Halder A, Tyo EC, Martinson ABF, et al. 2017. Copper cluster size effect in methanol synthesis from CO_2. *J. Phys. Chem. C* 121:10406–12
13. Kwon G, Ferguson GA, Heard CJ, Tyo EC, Yin C, et al. 2013. Size-dependent subnanometer Pd cluster (Pd_4, Pd_6, and Pd_{17}) water oxidation electrocatalysis. *ACS Nano* 7:5808–17
14. Winans RE, Vajda S, Ballentine GE, Elam JW, Lee B, et al. 2006. Reactivity of supported platinum nanoclusters studied by in situ GISAXS: clusters stability under hydrogen. *Top. Catal.* 39:145–49
15. Lee S, Lee B, Mehmood F, Seifert S, Libera JA, et al. 2010. Oxidative decomposition of methanol on subnanometer palladium clusters: the effect of catalyst size and support composition. *J. Phys. Chem. C* 114:10342–48
16. Molina LM, Lee S, Sell K, Barcaro G, Fortunelli A, et al. 2011. Size-dependent selectivity and activity of silver nanoclusters in the partial oxidation of propylene to propylene oxide and acrolein: a joint experimental and theoretical study. *Catal. Today* 160:116–30
17. Abbet S, Sanchez A, Heiz U, Schneider W-D, Ferrari AM, et al. 2000. Acetylene cyclotrimerization on supported size-selected Pd_n clusters ($1 \leq n \leq 30$): One atom is enough! *J. Am. Chem. Soc.* 122:3453–57
18. Roldán A, Ricart JM, Illas F, Pacchioni G. 2010. O_2 activation by Au_5 clusters stabilized on clean and electron-rich MgO stepped surfaces. *J. Phys. Chem. C* 114:16973–78
19. Moses-DeBusk M, Yoon M, Allard LF, Mullins DR, Wu Z, et al. 2013. CO oxidation on supported single Pt atoms: experimental and ab initio density functional studies of CO interaction with Pt atom on θ-Al_2O_3(010) surface. *J. Am. Chem. Soc.* 135:12634–45
20. Rondelli M, Zwaschka G, Krause M, Rötzer MD, Hedhili MN, et al. 2017. Exploring the potential of different-sized supported subnanometer Pt clusters as catalysts for wet chemical applications. *ACS Catal.* 7:4152–62
21. Whetten RL, Cox DM, Trevor DJ, Kaldor A. 1985. Correspondence between electron binding energy and chemisorption reactivity of iron clusters. *Phys. Rev. Lett.* 54:1494–97
22. Holmgren L, Andersson M, Rosen A. 1995. CO reactivity of small transition metal clusters: Ni_n and Nb_n. *Surf. Sci.* 331:231–36
23. Bérces A, Hackett PA, Lian L, Mitchell SA, Rayner DM. 1998. Reactivity of niobium clusters with nitrogen and deuterium. *J. Chem. Phys.* 108:5476–90
24. Parks EK, Nieman GC, Kerns KP, Riley SJ. 1998. The thermodynamics of nitrogen adsorption on nickel clusters: Ni_{19}–Ni_{71}. *J. Chem. Phys.* 108:3731–39
25. Icking-Konert GS, Handschuh H, Ganteför G, Eberhardt W. 1996. Bonding of CO to metal particles: photoelectron spectra of $Ni_n(CO)_m^-$ and $Pt_n(CO)_m^-$ clusters. *Phys. Rev. Lett.* 76:1047–50
26. Duncan MA. 2012. Laser vaporization cluster sources. *Rev. Sci. Instrum.* 83:041101–119
27. Pearmain D, Park SJ, Wang ZW, Abdela A, Palmer RE, Li ZY. 2013. Size and shape of industrial Pd catalyst particles using size-selected clusters as mass standards. *Appl. Phys. Lett.* 102:163103–107
28. Yin F, Wang ZW, Palmer RE. 2011. Controlled formation of mass-selected Cu-Au core-shell cluster beams. *J. Am. Chem. Soc.* 133:10325–27
29. Pratontep S, Carroll SJ, Xirouchaki C, Streun M, Palmer RE. 2005. Size-selected cluster beam source based on radio frequency magnetron plasma sputtering and gas condensation. *Rev. Sci. Instrum.* 76:045103–111
30. Ganteför G, Siekmann HR, Lutz HO, Meiwes-Broer KH. 1990. Pure metal and metal-doped rare-gas clusters grown in a pulsed-arc cluster ion-source. *Chem. Phys. Lett.* 165:293–96

31. de Heer WA. 1993. The physics of simple metal clusters: experimental aspects and simple models. *Rev. Mod. Phys.* 65:611–76
32. Popok VN, Barke I, Campbell EEB, Meiwes-Broer K-H. 2011. Cluster-surface interaction: from soft landing to implantation. *Surf. Sci. Rep.* 66:347–77
33. Wegner K, Piseri P, Tafreshi HV, Milani P. 2006. Cluster beam deposition: a tool for nanoscale science and technology. *Phys. D Appl. Phys.* 39:R439–59
34. Bromann K, Fèlix C, Brune H, Harbich W, Monot R, et al. 1996. Controlled deposition of size-selected silver nanoclusters. *Science* 274:956–58
35. Tyo EC, Vajda S. 2015. Catalysis by clusters with precise number of atoms. *Nat. Nanotech.* 10:577–588
36. Heiz U, Vanolli F, Trento L, Schneider W-D. 1997. Chemical reactivity of size-selected supported clusters: an experimental setup. *Rev. Sci. Instrum.* 68:1986–94
37. Vajda S, White MG. 2015. Catalysis applications of size-selected cluster deposition. *ACS Catal.* 5:7152–76
38. Schouteden K, Lauwaet K, Janssens E, Barcaro G, Fortunelli A, et al. 2014. Probing the atomic structure of metallic nanoclusters with the tip of a scanning tunneling microscope. *Nanoscale* 6:2170–76
39. Roberts FS, Anderson SL, Reber AC, Khanna SN. 2015. Initial and final state effects in the ultraviolet and X-ray photoelectron spectroscopy (UPS and XPS) of size-selected Pd_n clusters supported on TiO_2(110). *J. Phys. Chem. C* 119:6033–46
40. Bonanni S, Aït-Mansour K, Harbich W, Brune H. 2012. Effect of the TiO_2 reduction state on the catalytic CO oxidation on deposited size-selected Pt clusters. *J. Am. Chem. Soc.* 134:3445–50
41. Kaden WE, Wu T, Kunkel WA, Anderson SL. 2009. Electronic structure controls reactivity of size-selected Pd clusters adsorbed on TiO_2 surfaces. *Science* 326:826–29
42. Haruta M, Kobayashi T, Sano H, Yamada N. 1987. Novel gold catalysts for the oxidation of carbon monoxide at a temperature far below 0°C. *Chem. Lett.* 16:405–8
43. Hvolbæk B, Janssens TVW, Clausen BS, Falsig H, Christensen CH, Nørskov JK. 2007. Catalytic activity of Au nanoparticles. *Nano Today* 2:14–18
44. Sanchez A, Abbet S, Heiz U, Schneider W-D, Häkkinen H, et al. 1999. When gold is not noble: nanoscale gold catalysts. *J. Phys. Chem. A* 103:9573–78
45. Herzing AA, Kiely CJ, Carley AF, Landon P, Hutchings GJ. 2008. Identification of active gold nanoclusters on iron oxide supports for CO oxidation. *Science* 321:1331–35
46. Lee S, Molina LM, Lopez MJ, Alonso JA, Hammer B, et al. 2009. Selective propene epoxidation on immobilized $Au_{6–10}$ clusters: the effect of hydrogen and water on activity and selectivity. *Angew. Chem. Int. Ed.* 48:1467–71
47. Yang Z, Wu R, Goodman DW. 2000. Structural and electronic properties of Au on TiO_2(110). *Phys. Rev. B* 61:14066–6071
48. Heiz U, Sanchez A, Abbet S, Schneider W-D. 1999. Catalytic oxidation of carbon monoxide on monodispersed platinum clusters: Each atom counts. *J. Am. Chem. Soc.* 121:3214–17
49. Crampton SA, Rötzer MD, Ridge CJ, Schweinberger FF, Heiz U, et al. 2016. Structure sensitivity in the nanoscalable regime explored via catalyzed ethylene hydrogenation on supported platinum clusters. *Nat. Comm.* 7:10389–400
50. Keppeler M, Braugnin G, Radhakrishnan SG, Liu X, Jensen C, Roduner E. 2016. Reactivity of diatomics and of ethylene on zeolite-supported 13-atom platinum nanoclusters. *Cat. Sci. Technol.* 6:6814–23
51. Vajda S, Pellin MJ, Greeley JP, Marshall CL, Curtiss LA, et al. 2009. Subnanometre platinum clusters as highly active and selective catalysts for the oxidative dehydrogenation of propane. *Nat. Mater.* 8:213–16
52. Watanabe Y, Wu X, Hirata H, Isomura N. 2011. Size-dependent catalytic activity and geometries of size-selected Pt clusters on TiO_2(110) surfaces. *Catal. Sci. Technol.* 1:1490–95
53. Yang C-T, Wood BC, Bhethanabotla VR, Joseph B. 2015. The effect of the morphology of supported subnanometer Pt clusters on the first and key step of CO_2 photoreduction. *Phys. Chem. Chem. Phys.* 17:25379–92
54. Yang C-T, Wood BC, Bhethanabotla VR, Joseph B. 2014. CO_2 adsorption on anatase TiO_2(101) surfaces in the presence of subnanometer Ag/Pt clusters: implications for CO_2 photoreduction. *J. Phys. Chem. C* 118:26236–48

55. Baxter ET, Ha M-A, Alexandrova AN, Anderson SL. 2017. Ethylene dehydrogenation on $Pt_{4,7,8}$ clusters on Al_2O_3: strong cluster-size dependence linked to preferred catalyst morphologies. *ACS Catal.* 7:3322–35
56. Zhai H, Alexandrova AN. 2016. Ensemble-average representation of Pt clusters in conditions of catalysis accessed through GPU accelerated deep neural network fitting global optimization. *J. Chem. Theory Comput.* 12:6213–26
57. Zhai H, Alexandrova AN. 2017. Fluxionality of the clusters. When it matters and how to address it. *ACS Catal.* 7:1905–11
58. Alexandrova AN, Boldyrev AI. 2005. Search of the $Li_n^{0/+1/-1}$ ($n = 5$–7) lowest-energy structures using the ab-initio gradient embedded genetic algorithm (GEGA). Elucidation of the chemical bonding in the lithium clusters. *J. Chem. Theory Comput.* 1:566–80
59. Alexandrova AN. 2010. $(H_2O)_n$ clusters: microsolvation of the hydrogen atom via molecular ab initio gradient embedded genetic algorithm (GEGA). *J. Phys. Chem. A* 114:12591–99
60. Kanters RPF, Donald KJ. 2014. CLUSTER: searching for unique low energy minima of structures using a novel implementation of a genetic algorithm. *J. Chem. Theory Comput.* 10:5729–37
61. Davis J, Shayegui A, Horswell SL, Johnston RL. 2015. The Birmingham parallel genetic algorithm and its application to the direct DFT global optimization of Ir_N ($N = 10$–20) clusters. *Nanoscale* 7:14032–38
62. Bandow B, Hartke B. 2006. Larger water clusters with edges and corners on their way to ice: structural trends elucidated with an improved parallel evolutionary algorithm. *J. Phys. Chem. A* 110:5809–22
63. Jimenez-Izal E, Mercero JM, Matxain JM, Audiffred M, Moreno D, et al. 2014. Doped aluminum cluster anions: Size matters. *J. Phys. Chem. A* 118:4309–14
64. Wang J, Ma L, Zhao J, Jackson KA. 2009. Structural growth behavior and polarizability of Cd_nTe_n ($n = 1$–14) clusters. *J. Chem. Phys.* 130:214307
65. Call ST, Zubarev DY, Boldyrev AI. 2007. Global optimization searches via particle swarm optimization. *J. Comput. Chem.* 28:1177–86
66. Avendaño-Franco G, Romero AH. 2016. Firefly algorithm for structural search. *J. Chem. Theory Comput.* 12:3416–28
67. Zhai H-J, Zhao Y-F, Li W-L, Chen Q, Hu H-S, et al. 2014. Observation of an all-boron fullerene. *Nat. Chem.* 6:727–31
68. Sumpter BG, Noid DW. 1992. Potential energy surfaces for macromolecules. A neural network technique. *Chem. Phys. Lett.* 192:455–62
69. Zhai H, Ha M-A, Alexandrova AN. 2015. AFFCK: adaptative force-field-assisted ab initio coalescence kick method for global minimum search. *J. Chem. Theory Comput.* 11:2385–93
70. Hussein HA, Davis JBA, Johnston RL. 2016. DFT global optimisation of gas-phase and MgO-supported sub-nanometre AuPd clusters. *Phys. Chem. Chem. Phys.* 18:26133–43
71. Vilhelmsen LB, Hammer B. 2012. Systematic study of Au_6 to Au_{12} gold clusters on MgO(100) F centers using density-functional theory. *Phys. Rev. Lett.* 108:126101–105
72. Ha M-A, Baxter ET, Cass AC, Anderson SL, Alexandrova AN. 2017. Boron switch for selectivity of catalytic dehydrogenation on size-selected Pt clusters on Al_2O_3. *J. Am. Chem. Soc.* 139:11568–75
73. Li L, Wang L-L, Johnson DD, Zhang Z, Sanchez SI, et al. 2013. Noncrystalline-to-crystalline transformations in Pt nanoparticles. *J. Am. Chem. Soc.* 135:13062–72
74. Li Y, Zakharov D, Zhao S, Tappero R, Jung U, et al. 2015. Complex structural dynamics of nanocatalysts revealed in operando conditions by correlated imaging and spectroscopy probes. *Nat. Commun.* 6:7583
75. Mager-Maury C, Bonnard G, Chizallet C, Sautet P, Raybaud P. 2011. H_2-induced reconstruction of supported Pt clusters: metal-support interaction versus surface hydride. *ChemCatChem* 3:200–7
76. Negreiros FR, Fabris S. 2014. Role of cluster morphology in the dynamics and reactivity of subnanometer Pt clusters supported on ceria surfaces. *J. Phys. Chem. C* 118:21014–20
77. Sterrer M, Freund H-J. 2013. Towards realistic surface science models of heterogeneous catalysts: influence of support hydroxylation and catalyst preparation method. *Catal. Lett.* 143:375–85
78. Pacchioni G. 2013. Electronic interactions and charge transfer of metals atoms and cluster oxide surfaces. *Phys. Chem. Chem. Phys.* 15:1737–57
79. Jia C, Fan W. 2015. A theoretical study of O_2 activation by the Au_7-cluster on $Mg(OH)_2$: roles of surface hydroxyl defects. *Phys. Chem. Chem. Phys.* 17:30736–743

80. Liu J-C, Tang Y, Chang C-R, Wang Y-G, Li J. 2016. Mechanistic insights into propene epoxidation with O_2-H_2O mixture on Au_7/α-Al_2O_3: a hydroproxyl pathway from ab initio molecular dynamics simulations. *ACS Catal.* 6:2525–35
81. Addou R, Senftle TP, O'Connor N, Janik MJ, van Duin ACT, Bratzill M. 2014. Influence of hydroxyls on Pd atom mobility and clustering on rutile TiO_2(011)-2 x 1. *ACS Nano* 8:6321–33
82. Berdala J, Freund E, Lynch J. 1986. Environment of platinum atoms in a H_2PtCl_6/Al_2O_3 catalyst: influence of metal loading and chlorine content. *J. Phys. Colloq.* 47:269–70
83. Marger-Maury C, Chizallet C, Sautet P, Raybaud P. 2012. Platinum nanoclusters stabilized on γ-alumina by chlorine used as a capping surface ligand: a density functional theory study. *ACS Catal.* 2:1346–57
84. Campbell CT. 2012. Catalyst-support interactions: electronic perturbations. *Nat. Chem.* 4:597–98
85. Negreiros FR, Barcaro G, Sementa L, Fortunelli A. 2014. Concepts in theoretical heterogeneous ultra-nanocatalysis. *C. R. Chim.* 17:625–33
86. Mammen N, Gironcoli S, Narasimhan S. 2015. Substrate doping: a strategy for enhancing reactivity on gold nanocatalysts by tuning sp bands. *J. Chem. Phys.* 143:144307–312
87. Tauster SJ, Fung SC, Garten RL. 1978. Strong metal–support interactions. Group 8 noble metals supported on titanium dioxide. *J. Am. Chem. Soc.* 100:170–75
88. Tauster SJ. 1987. Strong metal–support interactions. *Acc. Chem. Res.* 20:389–94
89. Bruix A, Rodríguez JA, Ramírez PJ, Senayasake SD, Evans J, et al. 2012. A new type of strong metal–support interaction and the production of H_2 through transformation of water on Pt/CeO_2(111) and Pt/CeO_x/TiO_2(110) catalysts. *J. Am. Chem. Soc.* 134:8968–74
90. Carrasco J, López-Durán D, Zongyuan L, Duchoň T, Evans J, et al. 2015. In situ and theoretical studies for the dissociation of water on an active Ni/CeO_2 catalyst: importance of strong metal–support interactions for the cleavage of O–H bonds. *Angew. Chem. Int. Ed.* 54:3917–21
91. Bliem R, Hoeven JVD, Zavodny A, Gamba O, Pavelec J, et al. 2015. An atomic-scale view of CO and H_2 oxidation on a Pt/Fe_3O_4 model catalyst. *Angew. Chem. Int. Ed.* 54:13999–4002
92. Yoon B, Häkkinen H, Landman U, Wörz AS, Antonietti J-M, et al. 2005. Charging effects on bonding and catalyzed oxidation of CO on Au_8 clusters on MgO. *Science* 307:403–7
93. Ma L, Melnader M, Weckman T, Laasome K, Akola J. 2016. CO oxidation on the $Au_{15}Cu_{15}$ cluster and the role of vacancies in the MgO(100) support. *J. Phys. Chem. C* 120:26747–58
94. Kalhara GT, Seebauer EG, Saeys M. 2017. Ethylene hydrogenation over Pt/TiO_2. A charge-sensitive reaction. *ACS Catal.* 7:1966–70
95. Schlexer P, Ruiz Puigdollers A, Pacchioni G. 2015. Tuning the charge state of Ag and Au atoms and clusters deposited on oxide surfaces by doping: a DFT study of the adsorption properties of nitrogen- and niobium-doped TiO_2 and ZrO_2. *Phys. Chem. Chem. Phys.* 17:22342–60
96. Buendia F, Vargas JA, Beltrán MR, Davis JBA, Johnston RL. 2016. A comparative study of Au_mRh_n ($4 \leq m + n \leq 6$) clusters in the gas phase versus those deposited on (100) MgO. *Phys. Chem. Chem. Phys.* 18:22122–28
97. Shen L, Dadras J, Alexandrova AN. 2014. Pure and Zn-doped Pt clusters go flat and upright on MgO(100). *Phys. Chem. Chem. Phys.* 16:26436–42
98. Dadras J, Shen L, Alexandrova AN. 2015. Pt-Zn clusters on MgO(100) and TiO_2(110): dramatically different sintering behavior. *J. Phys. Chem. C* 119:6047–55
99. Hu CH, Chizallet C, Mager-Maury C, Corral-Vallejo M, Sautet P, et al. 2010. Modulation of catalyst particle structure upon support hydroxylation: ab initio insights into Pd_{13} and Pt_{13}/γ-Al_2O_3. *J. Catal.* 274:99–110
100. Li J, Li X, Zhai H, Wang LS. 2003. Au_{20}: a tetrahedral cluster. *Science* 299:864–67
101. Gao Y, Shao N, Pei Y, Chen Z, Zeng XC. 2011. Catalytic activities of subnanometer gold clusters (Au_{16}–Au_{18}, Au_{20}, and Au_{27}–Au_{35}) for CO oxidation. *ACS Nano* 5:7818–29
102. Zhang C, Yoon B, Landman U. 2007. Predicted oxidation of CO catalyzed by Au nanoclusters on a thin defect-free MgO film supported on a Mo(100) surface. *J. Am. Chem. Soc.* 129:2228–29
103. Harding C, Habibpour V, Kunz S, Antonietti J-M, Farnbacher AN-S, et al. 2009. Control and manipulation of gold nanocatalysis: effects of metal oxide support thickness and composition. *J. Am. Chem. Soc.* 131:538–48

104. Ricci D, Bongiorno A, Pacchioni G, Landman U. 2006. Bonding trends and dimensionality crossover of gold nanoclusters on metal-supported MgO thin films. *Phys. Rev. Lett.* 97:036106–110
105. Yin C, Negreiros FR, Barcaro G, Beniya A, Sementa L, et al. 2017. Alumina-supported sub-nanometer Pt_{10} clusters: amorphization and role of the support material in a highly active CO oxidation catalyst. *J. Mater. Chem. A* 5:4923–31
106. Adiga SP, Zapol P, Curtiss LA. 2006. Atomistic simulations of amorphous alumina surfaces. *Phys. Rev. B* 74:064204
107. Adiga SP, Zapol P, Curtiss LA. 2007. Structure and morphology of hydroxylated amorphous alumina surfaces. *J. Phys. Chem. C* 111:7422–29
108. Ewing CS, Bhavsar S, Veser G, McCarthy JJ, Johnson JK. 2014. Accurate amorphous silica surface models from first-principles thermodynamics of surface dehydroxylation. *Langmuir* 30:5133–41
109. Cheng L, Yin C, Mehmood F, Liu B, Greeley J, et al. 2014. Reaction mechanism for direct propylene epoxidation by alumina/supported silver aggregates: the role of the particle/support interface. *ACS Catal.* 4:32–39
110. Ewing CS, Hartmann MJ, Martin KR, Musto AM, Padinjarekutt SJ, et al. 2015. Structural and electronic properties of Pt_{13} nanoclusters on amorphous silica supports. *J. Phys. Chem. C* 119:2503–12
111. Mammen N, Narasimhan S, Gironcoli S. 2011. Tuning the morphology of gold clusters by substrate doping. *J. Am. Chem. Soc.* 133:2801–3
112. Yamijala SSRKC, Bandyopadhyay A, Pati SK. 2014. Nitrogen-doped graphene quantum dots as possible substrates to stabilize planar conformer of Au_{20} over its tetrahedral conformer: a systematic DFT study. *J. Phys. Chem. C* 118:17890–94
113. Yoon B, Landman U. 2008. Electric field control of structure, dimensionality, and reactivity of gold nanoclusters on metal-supported MgO films. *Phys. Rev. Lett.* 100:056102–106
114. Mondal K, Kamal C, Banerjee A, Chakrabarti A, Ghanty TK. 2015. Silicene: a promising surface to achieve morphological transformation in gold clusters. *J. Phys. Chem. C* 119:3192–98
115. Lee S, Lee B, Seifert S, Winans RE, Vajda S. 2015. Fischer–Tropsch synthesis at a low pressure on subnanometer cobalt oxide clusters: the effect of cluster size and support on activity and selectivity. *J. Phys. Chem. C* 19:11210–16
116. Cheng L, Yin C, Mehnood F, Liu B, Greeley J, et al. 2014. Reaction mechanism for direct propylene epoxidation by alumina-supported silver aggregates: the role of the particle/support interface. *ACS Catal.* 4:32–39
117. Hansen TW, Delariva AT, Challa SR, Dayte AK. 2013. Sintering of catalytic nanoparticles: particle migration or Ostwald ripening? *Acc. Chem. Rev.* 46:1720–30
118. Ostwald W, ed. 1893. *Lehrbuch der Allgemeinen Chemie*, Vol. 2, Part 1. Leipzig, Ger.: Engelmann
119. Yang F, Chen MS, Goodman DW. 2009. Sintering of Au particles supported on TiO_2(110) during CO oxidation. *J. Phys. Chem. C* 113:254–60
120. Kang SB, Lim JB, Jo D, Cho BK, Hong SB, et al. 2017. Ostwald-ripening sintering kinetics of Pd-based three-way catalyst: importance of initial particle size of Pd. *Chem. Eng. J.* 316:631–44
121. Bayram E, Lu J, Aydin C, Browning ND, Özkar S, et al. 2015. Agglomerative sintering of an atomically dispersed Ir_1/zeolite Y catalyst: compelling evidence against Ostwald ripening but for bimolecular and autocatalytic agglomeration catalyst sintering steps. *ACS Catal.* 5:3514–27
122. Aydin C, Lu J, Browning ND, Gates BC. 2012. A "smart" catalyst: sinter-resistant supported iridium clusters visualized with electron microscopy. *Angew. Chem. Int. Ed.* 51:5929–34
123. Fukamori Y, König M, Yoon B, Wang B, Esch F, et al. 2013. Fundamental insight into the substrate-dependent ripening of monodisperse clusters. *ChemCatChem* 5:3330–41
124. Farmer JA, Campbell CT. 2010. Ceria maintains smaller metal catalyst particles by strong metal-support binding. *Science* 329:933–36
125. Berg RVD, Parmentier TE, Elkjær CF, Gommes CJ, Sehested J, et al. 2015. Support functionalization to retard Ostwald ripening in copper methanol synthesis catalysts. *ACS Catal.* 5:4439–48
126. Tian Y, Liu Y-J, Zhao J-X, Ding Y-D. 2015. High stability and superior catalytic reactivity of nitrogen-doped graphene supporting Pt nanoparticles as a catalyst for the oxygen reduction reaction: a density functional theory study. *RSC Adv.* 5:34070–77

127. Koizumi K, Nobusada K, Boero M. 2017. Simple but efficient method for inhibiting sintering and aggregation for catalytic Pt nanoclusters on metal-oxide support. *Chem. Eur. J.* 23:1531–38
128. Ferguson GA, Yin C, Kwon G, Tyo EC, Lee S, et al. 2012. Stable subnanometer cobalt oxide clusters on ultrananocrystalline diamond and alumina support: oxidation state and the origin of sintering resistance. *J. Phys. Chem. C* 116:24027–34
129. Dadras J, Jimenez-Izal E, Alexandrova AN. 2015. Alloying Pt sub-nano-clusters with boron: sintering preventative and coke antagonist? *ACS Catal.* 5:5719–27
130. Wettergren K, Schweinberger FF, Deiana D, Ridge CJ, Crampton AS, et al. 2014. High sintering resistance of size-selected platinum cluster catalysts by suppressed Ostwald ripening. *Nano Lett.* 14:5803–9
131. Graham GW, Jen H-W, Ezekoye O, Kudla RJ, Chun W, et al. 2007. Effect of alloy composition on dispersion stability and catalytic activity for NO oxidation over alumina-supported Pt-Pd catalysts. *Catal. Lett.* 116:1–8
132. Ha M-A, Dadras J, Alexandrova AN. 2014. Rutile-deposited Pt-Pd clusters: a hypothesis regarding the stability at 50/50 ratio. *ACS Catal.* 4:3570–80
133. Bliem R, van der Hoeven JES, Hulva J, Jiri P, Gamba O, et al. 2016. Dual role of CO in the stability of subnano Pt clusters at the $Fe_3O_4(001)$ surface. *PNAS* 113:8921–23
134. Podda N, Corva M, Mohamed F, Feng Z, Dri C, et al. 2017. Experimental and theoretical investigation of the restructuring process induced by CO at near ambient pressure: Pt nanoclusters on graphene/Ir(111). *ACS Nano* 11:1041–53
135. Abidi PTZ, Zhdanov VP, Langhammer C, Grönbeck H. 2015. Transient bimodal particle size distributions during Pt sintering on alumina and silica. *J. Phys. Chem. C* 119:989–96
136. Martin ET, Gai PL, Boyes ED. 2015. Dynamic imaging of Ostwald ripening by environmental scanning transmission electron microscopy. *ChemCatChem* 7:3705–11
137. Plessow PN, Abild-Pedersen F. 2016. Sintering of Pt nanoparticles via volatile PtO_2: simulation and comparison with experiments. *ACS Catal.* 6:7098–108
138. Negreiros FR, Aprà E, Barcaro G, Sementa L, Vajda S, Fortunelli A. 2012. A first-principles theoretical approach to heterogeneous nanocatalysis. *Nanoscale* 4:1208–19
139. Barcaro G, Fortunelli A. 2007. A magic Pd-Ag binary cluster on the F_s-defected MgO(100) surface. *J. Phys. Chem. C* 111:11384–89
140. Vargas A, Santarossa G, Iannuzzi M, Baiker A. 2009. Fluxionality of gold nanoparticles investigated by Born–Oppenheimer molecular dynamics. *Phys. Rev. B* 80:195421
141. Li J, Yin D, Chen C, Li Q, Lin L, et al. 2015. Atomic-scale observation of dynamical fluctuation and three-dimensional structure of gold clusters. *J. Appl. Phys.* 117:085303
142. Häkkinen H, Abbet S, Sanchez A, Heiz U, Landman U. 2003. Structural, electronic, and impurity-doping effects in nanoscale chemistry supported gold nanoclusters. *Angew. Chem. Int. Ed.* 42:1297–300
143. Liu L, Liu Z, Sun H, Zhao Z. 2017. Morphological effects of Au_{13} clusters on the adsorption of CO_2 over anatase $TiO_2(101)$. *Appl. Surf. Sci.* 399:469–79
144. Pidko EA. 2017. Toward the balance between the reductionist and systems approaches in computational catalysis: model versus method accuracy for the description of catalytic systems. *ACS Catal.* 7:4230–34
145. Krcha MD, Janik MJ. 2014. Challenges in the use of density functional theory to examine catalysis by M-doped ceria surfaces. *Int. J. Quant. Chem.* 114:8–13
146. Pacchioni G. 2008. Modeling doped and defective oxides in catalysis with density functional theory methods: room for improvements. *J. Chem. Phys.* 128:182505
147. Chen GP, Voora VK, Agee MM, Balasubrabani SG, Furche F. 2017. Random-phase approximation methods. *Annu. Rev. Phys. Chem.* 68:421–45
148. Cui Z-H, Wu F, Jiang H. 2016. First-principles study of relative stability of rutile and anatase TiO_2 using the random phase approximation. *Phys. Chem. Chem. Phys.* 18:29914–22
149. Anisimov VI, Korotin MA, Kurmaev EZ. 1990. Band-structure description of Mott insulators (NiO, MnO, FeO, CoO). *J. Phys. Condens. Matter* 2:3973–87
150. Anisimov VI, Gunnarsson O. 1991. Density-functional calculation of effective Coulomb interactions in metals. *Phys. Rev. B* 43:7570–74

151. Kulik HJ, Cococcioni M, Scherlis DA, Marzari N. 2006. Density functional theory in transition-metal chemistry: a self-consistent Hubbard *U* approach. *Phys. Rev. Lett.* 97:103001
152. Hsu H, Umemoto K, Cococcioni M, Wentzcovitch R. 2009. First-principles study for low-spin $LaCoO_3$ with a structurally consistent Hubbard *U*. *Phys. Rev. B* 79:125124
153. Heyd J, Scuseria GE, Ernzerhof M. 2003. Hybrid functionals based on a screened Coulomb potential. *J. Chem. Phys.* 118:8207–15
154. Rusakov AA, Zgid D. 2016. Second-order Green's function perturbation theory for periodic systems. *J. Chem. Phys.* 144:054106–120